JHC ex*PRESS*
Online publication date May 30, 2005
This article may be cited as DOI: 10.1369/jhc.4A6592.2005

Running headline:

PAR_4 ACTIVATION AND ACTIN FIBER FORMATION

Activation of PAR_4 Induces a Distinct Actin Fiber Formation via p38 MAPK in Human Lung Endothelial Cells

Masakazu Fujiwara, Enjing Jin, Mohammad Ghazizadeh and Oichi Kawanami

Department of Molecular Pathology, Nippon Medical School,
Graduate School of Medicine, Institute of Gerontology

Address all correspondence to:

Oichi Kawanami, M.D., Ph. D.
Department of Molecular Pathology, Nippon Medical School,
Graduate School of Medicine, Institute of Gerontology
1-396 Kosugi-cho, Nakahara-ku, Kawasaki, Kanagawa,
Japan, 211-8533.

Tel: +81-44-733-1823
Fax: +81-44-733-1293
E-mail: kawanami@nms.ac.jp

Received for publication December 2, 2004; accepted March 23, 2005 [DOI:

10.1369/jhc.4A6592.2005].

JHC ex*PRESS*
Online publication date May 30, 2005
This article may be cited as DOI: 10.1369/jhc.4A6592.2005

SUMMARY

Protease-activated receptors (PARs) are multi-functional G-protein coupled receptors. Among the four existing PARs, PAR_4 is preferentially expressed in the human lung tissue. However, the function of PAR_4 has not been defined in the lung endothelial cells. Since PAR_1-mediated cellular effects are deeply related to the morphological changes, we focused on the actin fiber and p38 MAPK signaling involved in actin polymerization to elucidate the role of PAR_4. RT-PCR and Western blot analyses identified PAR_4 expression in human pulmonary artery endothelial cells (HPAEC) and in human microvascular endothelial cells from lung (HMVEC-L). We then examined the changes in actin fibers in endothelial cells treated with PAR_4 activating peptide (GYPGQV). PAR_1 activating peptide (SFLLRN) was used for comparison. Activation of PAR_4 and PAR_1 by their corresponding peptides induced actin fiber formation, however, the actin filaments were broadly bundled in PAR_4 as compared to the ring like actin filaments in PAR_1 activation. Correspondingly, the magnitude of p38 MAPK phosphorylation was different between cells treated with PAR_4 and PAR_1, with PAR_4 activating peptide showing a significantly higher sensitivity to p38 MAPK inhibitor, SB203580. Taken together, these results demonstrate that activation of PAR_4 results in the formation of actin fiber distinct from that by PAR_1 activation, suggesting PAR_4 may play specific roles in the lung endothelial cells.

KEY WORDS: pulmonary endothelial cells; G-protein coupled receptors; protease-activated receptor; thrombin; actin; p38 MAPK

JHC ex*PRESS*
Online publication date May 30, 2005
This article may be cited as DOI: 10.1369/jhc.4A6592.2005

Introduction

Protease-activated receptors (PARs) are cell surface receptors that mediate signals to G proteins (Vu et al. 1991). To date, four PARs, including PAR_1 (Vu et al. 1991), PAR_2 (Nystedt et al. 1995), PAR_3 (Ishihara et al. 1997), and PAR_4 (Xu et al. 1998) have been reported. These receptors, with putative seven transmembrane domains, are activated by a number of serine proteases, such as thrombin (Carney et al. 1992), trypsin (Nystedt et al. 1994), mast cell tryptase (Molino et al. 1997), and factor Xa (Kawabata et al. 2001) at the unique cleavage site of PARs. The newly formed amino terminal of PARs, called tethered ligand, then intramolecularly activates itself, and transmits the signals into cells (Bahou et al. 1994; Gerszten et al. 1994). Furthermore, PARs can be activated by synthetic peptides corresponding to each receptor's tethered ligand (Lan et al. 2000).

Stimulation of PARs is known to induce a variety of cellular effects in many types of cells. In the endothelial cells, for example, PAR_1 upregulated cyclooxygenase-2 expression (Houliston et al. 2002), intercellular adhesion molecule (ICAM)-1 transcription (Rahman et al. 2002), and PAR_2 induced tissue factor expression and von Willebrand factor release (Langer et al. 1999). These results indicate the multi-functionality of these G-protein coupled receptors, and show the functional involvement of receptors in a number of events taken place in endothelial cell. However, functional analysis of PAR_4 has been limited to the studies in platelets, smooth muscle cells, and epithelial cells (Asokananthan et al. 2002; Bretschneider et al. 2001; Covic et al. 2002; Henriksen and Hanks 2002), but not in endothelial cells.

Previously, we have shown the preferential expression of PAR_4 in human lung vascular endothelial cells *in vitro* (Fujiwara et al. 2004). In PARs signaling, activation of

Online publication date May 30, 2005
This article may be cited as DOI: 10.1369/jhc.4A6592.2005

mitogen-activated protein kinase (MAPK) takes an important part in endothelial cell function (Kataoka et al. 2003; Marin et al. 2001). Among the MAPK family, p38 MAPK was shown to regulate actin cytoskeletal remodeling in pulmonary microvascular endothelial cells upon ICAM-1 ligation (Wang and Doerschuk 2001). Furthermore, remodeling of actin fibers was deeply involved in the major functions of endothelial cells, such as permeability (Kouklis et al. 2004), endothelium-dependent relaxation (Hamilton et al. 2001), cell migration (Vasanji et al. 2004), microtubele integrity (Bayless and Davis 2004), and leukocyte adherence (Vergnolle et al. 2002).

In this study, we investigated whether PAR_4 and PAR_1 play different roles in actin reorganization in human pulmonary artery endothelial cells (HPAEC) and human microvascular endothelial cells from lung (HMVEC-L), and whether the actin formation by elicitation of PAR_4 and/or PAR_1 is p38 MAPK-dependent in these human lung endothelial cells. Furthermore, we examined if PAR_4-induced actin fibers display different morphology from the PAR_1-induced actin fibers. The results indicated that the functional role of PAR_4 in lung endothelial cells involved actin fiber formation and the resulting morphology of the fibers differed from that derived from PAR_1 activation through a distinct signaling pathway.

This article may be cited as DOI: 10.1369/jhc.4A6592.2005

Materials and Methods

Reagents

Human α-thrombin was purchased from Sigma (St. Louis, MO). The anti- PAR_4 polyclonal goat antibody was from Santa Cruz (Santa Cruz, CA). The anti-p38 MAPK, anti-phospho-p38 MAPK, anti-Hsp27, and anti-phospho-Hsp27 antibodies were from Cell Signaling Technology Inc. (Beverly, MA). PAR_1 activating peptide, SFLLRN-0H, was from BACHEM (Budendorf, Switzerland) and PAR_4 activating peptide, GYPGQV-NH_2, and its scrambled peptide, YGPGQV-NH_2, were from BioGate Co., Ltd (Gifu, Japan). All the peptides used in the experiments were HPLC grade with >95% purity. Aminopeptidase inhibitor, amastatin, was from Peptide Institute, Inc. (Osaka, Japan).

Endothelial Cell Culture and Tissue Sections

HPAEC and HMVEC-L obtained from Clonetics (Walkersville, MD) were cultured in EBM medium (Clonetics) supplemented with EGM-MV singlequots. Cells were plated onto gelatin-coated flasks, and grown under 5% CO_2 at 37C°.

Formalin-fixed, paraffin-embedded tissue sections from human lung and lymph node were obtained from the surgical pathology division.

Immunohistochemistry

Tissue sections (4 μm) were deparaffinized in xylene and rehydrated in ethanol series. Endogenous peroxidase activity in the sections was blocked by 0.3% (v/v) hydrogen peroxide in distilled water for 10 min. To retrieve antigens, the sections were placed in an antigen retrieval medium (Immunosaver, Nissin EM Co., Ltd, Tokyo, Japan) and heated at 98C° for 1 h. After

This article may be cited as DOI: 10.1369/jhc.4A6592.2005

cooling down to the room temperature, nonspecific binding sites were inhibited by incubation with 1:10 normal rabbit serum for 30 min. The slides were then incubated overnight with a 1:50 dilution of polyclonal goat anti- PAR_4 antibody. The reaction product was visualized using the labeled streptavidin-biotin (LSAB) system (DAKO Japan) and 3, 3`diaminobenzidine as a chromogen, and the sections were counterstained with hematoxylin. Negative control sections were processed by substitution of the primary antibody with normal goat serum. The intensity of immunostaining was semiquantitated as: -, negative; +, weak; ++, moderate, and +++, strong.

Semiquantitative RT-PCR

Cultured endothelial cells were washed and then lysed in guanidine thiocyanate-containing buffer and total RNAs were extracted using the RNeasy Mini Kit (Qiagen, Hilden, Germany) with DNase I treatment. Semiquantitative RT-PCR for PAR_4 was performed as previously described (Fujiwara et al. 2004). The PCR was performed at 94 C° for 45 sec, 58 C° for 45 sec and 72 C° for 2 min. After 24 cycles of amplification, cDNA products were visualized with SYBR Green I (Molecular Probes, Eugene, Oreg., USA) and band images were captured using Molecular Imager FX. Signal intensity of PAR_4 was then quantitated by PDQuest software (Bio-Rad, Hercules, Calif., USA) and normalized to or against GAPDH signal intensity. Independent experiments were conducted 3 times. RT-PCR reaction with no SuperScript RNase H^- reverse transcriptase did not show any PCR products.

Western Blot Analysis for PAR_4 and p38 MAPK Activations

Endothelial cells were plated in 60 mm dishes to reach subconfluence. After treatments, cells were washed and lysed either in RIPA buffer for PAR_4 (PBS, 1% (v/v) NP-40, 0.5% (w/v)

sodium deoxycholate, 0.1% (w/v) SDS, 0.1 mg/ml PMSF, 50 μg/ml aprotinin) or in buffer for p38 MAPK and Hsp27 analysis (50 mM HEPES, pH7.4, 50 mM NaCl, 5 mM EDTA, 1% (v/v) Triton X-100, 10% (v/v) glycerol, 1 mM Na_3VO_4, 100 mM NaF, 10 mM sodium pyrophosphate, and 34 μg/ml Aprotinin). SDS-polyacrylamide gel electrophoresis (PAGE) was performed by loading samples (100 μg/lane for PAR_4 and 30 μg/lane for p38 MAPK and Hsp27) in 5-15% gradient gels. Protein was transferred electrophoretically to a polyvinyl difluoride (PVDF) membrane for 1 h. The membrane was incubated in TBS (10 mM Tris HCl, pH 8.0, and 150 mM NaCl) containing 10% fetal bovine serum (FBS) for 1 h and with TBS containing 0.05% (v/v) Tween 20, 10% FBS, and each primary polyclonal antibodies (1:100 for PAR_4, 1:300 for p38 MAPK, and 1:500 for Hsp27). After three washes with TBS containing 0.05% (v/v) Tween 20, the binding of the anti- PAR_4 antibody was detected with biotinylated anti-goat IgG and avidin:biotinylated enzyme complex (Vector, Burlingame, CA). Immunoreactive bands for p38 MAPK and Hsp27 were visualized by chemiluminescence (ECL Plus, Amersham Pharmacia) with anti-rabbit or mouse antibody-HRP (1:4000). Intensity of bands was analyzed by NIH Image, performed on a Macintosh computer using the public domain NIH Image program developed at the U.S. National Institutes of Health, which were available on the Internet at http://rsb.info.nih.gov/nih-image/. After quantifying the bands, signal intensities of phosphorylated p38 MAPK (pp38 MAPK) were normalized to or against p38 MAPK signal intensities, and fold increase in phosphorylation was calculated.

Actin Fluorescence Staining

HPAEC and HMVEC-L (2×10^4 cells/1.7 cm^2) were cultured in Lab-Tek II chamber slides (NUNC, Rochester, NY) coated with gelatin and grown for 3 to 4 days to attain confluence. Cells

were serum starved for 18 h before addition of α-thrombin (Birukova et al. 2004; Fujiwara et al. 2004), SFLLRN (Fujiwara et al. 2004; Vouret-Craviari et al. 1998), GYPGQV, or dH_2O in EBM medium (0.25% {w/v} BSA) with 5 □M amastatin. After exposure to the experimental conditions for indicated period of time, the cells were washed with HBSS and fixed with 10% (v/v) neutralized formalin solution and then permeabilized with 0.1% (v/v) Triton X-100. The actin filaments of cells were stained with Alexa 488-phalloidin (Molecular Probes, Eugene, OR) for 30 min at room temperature, washed three times with PBS, mounted with FluoroGuard (BIO RAD, Hercules, CA), and examined under a confocal laser scanning microscopy equipped with ×20 and ×40 objective lenses (Leica, Wetzlar, Germany). Independent experiments were conducted 3 times.

p38 MAPK Inhibition

In the p38 MAPK inhibitory experiments, cells were first pretreated with 2.5 μM SB203580 for 15 min. At 2.5 μM of concentration, SB203580 clearly suppressed GYPGQV (PAR_4 activator) induced actin fibers and thus this dose was used in the present study. After the pretreatment, various agents were applied to the cells in the presence of SB203580 (2.5 μM) or vehicle for indicated period of times. The analyses were done by actin fluorescence staining and Western blot as described above.

JHC ex*PRESS*
Online publication date May 30, 2005
This article may be cited as DOI: 10.1369/jhc.4A6592.2005

Results

Expression of PAR_4 in Human Lung Tissue

To assess *in vivo* status of PAR_4 expression in human lung, immunohistochemical staining for PAR_4 was applied on lung tissues. Distinct PAR_4 expression was observed in vascular endothelial cells, type II alveolar epithelial cells and some inflammatory cells. The endothelial cells in microvessels (Fig. 1A; arrow) showed a strong reaction for PAR_4 similar to that in the large vessels (Fig. 1B; arrow). On the other hand, PAR_4 expression was not detected in lymph node tissue stained in parallel (Fig. 1C), as was previously shown by Northern blot analysis (Xu et al. 1998).

Expression of PAR_4 in HPAEC and HMVEC-L

By a semi-quantitative RT-PCR, both HPAEC and HMVEC-L expressed PAR_4 mRNA (Fig. 2A), and the expression level in HMVEC-L (Fig. 2A, lane 2) showed 1.97 ± 0.01-fold increase over the expression level in HPAEC (Fig. 2A, lane 1).

Western blot analysis revealed the expression of PAR_4 in both HPAEC and HMVEC-L, with a more abundance in HMVEC-L (Fig. 2B, lane 2). The specificity of Western blot analysis was confirmed by detection of a weak PAR_4 band in human aortic endothelial cell corresponding to its mRNA level by RT-PCR (Fujiwara et al. 2004).

PAR_4 Activation and Induction of Actin Fiber Formation

When HPAEC were exposed to various concentrations of PAR_4 activating peptide, GYPGQV (20, 100, and 500 μM), for 30 min (Fig. 3), only subtle effects in the width of actin bundles were observed at 20 μM and 100 μM. However, the reaction at the concentration of 500 μM resulted

This article may be cited as DOI: 10.1369/jhc.4A6592.2005

in the formation of dense bundles of long actin filaments. Compared to the control cells treated with vehicle, actin bundles were thick and densely localized at the cell boundary.

Exposure of GYPGQV (500 μM) for 15 min induced actin bundles at the cell boundary in HPAEC (Fig. 4A) and in HMVEC-L (Fig. 4B). In HPAEC, GYPGQV treatment showed increase in the thickness of actin bundles. However, the fluorescence intensity in HPAEC was not as dense as that of 30 min treatment (See Fig. 3). In HMVEC-L, exposure of GYPGQV induced dense and thickened actin fibers with strong Alexa 488-phalloidin actin staining (Fig. 4B; GYPGQV, lower panels). YGPGQV (500 μM), a negative control scrambled peptide, did not alter the actin architecture in both HPAEC (Fig. 4A; YGPGQV) and HMVEC-L (Fig. 4B; YGPGQV), and showed similar cell cytoskeletons as in the control cells.

Change in actin architecture was also recognized in the lung endothelial cells, when the cells were treated with α-thrombin or PAR_1 activating agent, SFLLRN, for 15 min (Fig. 5). We used effective dose of α-thrombin (2 U/ml) or PAR1 activating peptide (100 μM) based on the results of previous studies (Fujiwara et al. 2004; Vouret-Craviari et al. 1998). Reorganized actin fiber in HPAEC (Fig. 5A) and HMVEC-L (Fig. 5B) was dense, and formed cortical rings of polymerized actin. Furthermore, the cortical actin fiber in SFLLRN (100 μM) treated cells was similar to that in α-thrombin (2 U/ml) treated cells. However, these cells showed different morphology from that of the cells activated with PAR_4. The PAR_1-activated cells were morphologically more contracted as evidenced by ring-like condensation of actin fibers that was different from actin polymerization localized at the cell boundary induced by PAR_4 activation.

Involvement of p38 MAPK Phosphorylation During PAR_4 Activation

Involvement of p38 MAPK, one of the MAPK members that regulate actin fiber formation,

This article may be cited as DOI: 10.1369/jhc.4A6592.2005

was examined in HPAEC and HMVEC-L. In HPAEC, 1.94 ± 0.11-fold increase in pp38 MAPK was detected in GYPGQV treated cells (Fig. 6A, lane 2) than in the control cells (Fig. 6A, lane 1). Negative control peptide, YGPGQV, had no effect on p38 MAPK phosphorylation (Fig. 6A, lane 3). The SFLLRN treated cells responded most strongly and showed 5.93 ± 0.74-fold increase in pp38 MAPK level (Fig. 6A, lane 4). Similar results were also observed in HMVEC-L (Fig. 6B). Here, the phosphorylated p38 MAPK level in GYPGQV treated cells (Fig. 6B, lane 2) was 2.45 ± 0.68-fold more than control (Fig. 6B, lane 1) or YGPGQV (Fig. 6B, lane 3) treated cells. And SFLLRN increased pp38 MAPK level to 12.54 ± 2.81-fold (Fig. 6B, lane 4). Changes in p38 MAPK phosphorylated state were most apparent at 15 min and 5 min after the treatments for HPAEC and HMVEC-L, respectively. The expression level of total p38 MAPK was similar in both HPAEC and HMVEC-L (Fig. 6, lower panel).

Suppression of PAR_4-induced Actin Fiber Formation by p38 MAPK Inhibitor SB203580

To validate the role of p38 MAPK in PAR_4-induced actin fiber formation, p38 MAPK inhibitor, SB203580, was used. At 2.5 μM of concentration, SB203580 suppressed GYPGQV (PAR_4 activator) induced actin fibers in HPAEC as evidenced by the decreased thickness in longitudinal axis (Fig. 7A). In contrast, SB203580 could not alter actin fibers in SFLLRN (PAR_1 activator) or α-thrombin treated cells at the same concentration. In the control cells, no significant effect on actin fibers was detected under the presence of SB203580.

Activity of p38 MAPK under the presence of SB203580 was also confirmed by p38 MAPK downstream target, Hsp27 (Fig. 7B). In GYPGQV-treated cells, the amount of phosphorylated Hsp27 (pHsp27) was significantly decreased under the presence of SB203580 at 2.5 μM. Similarly, 2.5 μM of SB203580 suppressed the phosphorylation state of Hsp27 in control and

JHC ex*PRESS*
Online publication date May 30, 2005
This article may be cited as DOI: 10.1369/jhc.4A6592.2005

SFLLRN treated cells, indicating the abolishment of MAPK activity of p38 MAPK in SB203580 treated cells. Also, the expression of Hsp27 was lower in GYPGQV treated cells (both with and without SB203580) than control and SFLLRN treated cells.

JHC ex*PRESS*
Online publication date May 30, 2005
This article may be cited as DOI: 10.1369/jhc.4A6592.2005

Discussion

In the present study, the expression of PAR_4 and its functional roles in the lung endothelial cells were investigated. We first demonstrated PAR_4 expression in the lung vascular endothelial cells with a heterogeneous expression pattern between large and small vessels. These results indicated the importance of PAR_4 in endothelial cells of lung vessels, especially microvessels. Secondly, we demonstrated the PAR_4 function which induced a distinct actin fiber formation in HPAEC and HMVEC-L. These newly formed long actin filaments with a broadened dense localization along the cell boundary were morphologically different from that of PAR_1 induced cortical rings of polymerized actin. Furthermore, PAR_4 and PAR_1 activated cells showed a difference in terms of p38 MAPK participation, as observed by p38 MAPK inhibition experiments using SB203580. These results suggested unique capabilities of PAR_4 that was not provided by PAR_1, and indicated important actin-related functions of PAR_4 in the lung vascular endothelial cells.

As determined by immunohistochemistry, PAR_4 was strongly expressed in the endothelial cells of human lung tissue while lymph node tissue was unreactive. This is consistent with the previous results showing a high expression of PAR_4 mRNA in human lung tissues and lack of detections in lymph node tissue (Xu et al. 1998). In addition, we found that PAR_4 was also expressed in the cultured cells of HPAEC and HMVEC-L, being higher in HMVEC-L. Since, our previous comparative study on PAR_4 mRNA expression among human endothelial cells from pulmonary artery, aorta (Fujiwara et al. 2004), and dermal microvessel (data not shown) also showed a preferential expression of PAR_4 mRNA in the lung endothelial cells, a functionally important role for PAR_4 was implicated in the lung endothelial cells, especially in the capillary endothelial cells.

JHC ex*PRESS*
Online publication date May 30, 2005
This article may be cited as DOI: 10.1369/jhc.4A6592.2005

The differences between PAR_4 and PAR_1 have been reported from diverse viewpoints. At the genome structure level, human PAR_4 was shown to be localized at 19p12, whereas other human PARs, PAR_{1-3}, formed gene cluster at 5q13 (Kahn et al. 1998a). At the signaling cascade level, differential couplings of PAR_1 and PAR_4 to G proteins have been suggested (Asokananthan et al. 2002; Faruqi et al. 2000). Likewise, at the phenotypical level, we showed differences between PAR_4 and PAR_1 induced actin fiber formations. The morphology of rearranged PAR_4 induced actin fibers was more broadened compared to tightened actin fibers induced by PAR_1 activation. It should be noted that our study has demonstrated the morphological consequences of PAR1 activation in ECs and we have not directly measured the expression levels of PAR1 mRNA and protein in parallel, although the data could be confirmatory to our findings.

The morphological difference between PAR_4 and PAR_1 in rearranged actin fibers points out distinct activation kinetics of PAR_4 from PAR_1 in endothelial cells. Consistent with our findings, different kinetics of PAR_4 were reported by others (Kahn et al. 1998b; Shapiro et al. 2000). For example, Shapiro *et al*. indicated that signals of PAR_4 shut off more slowly than PAR_1 in human platelets. Also, in the platelets, Kahn *et al*. indicated the requirement of higher concentration of thrombin for the activation of PAR_4. This higher concentration requirement was also observed in our experiments, i.e. 500 μM of PAR_4 activating peptide (GYPGQV) was needed to induce dense and thickened bundles of long filaments, whereas only 100 μM of PAR_1 activating peptide (SFLLRN) was required to induce ring-like actin structures. These differences in activation kinetics indicated the unique and different roles of PAR_4, which was not provided by PAR_1.

The observation that PAR_4 induced actin fiber formation was highly sensitive to p38 MAPK inhibitor, SB203580, raised a hypothesis that p38 MAPK could be the principal factor which controls the diverse PARs-actin traffic pathways. In cardiomyocytes, PAR_4 was shown to activate

This article may be cited as DOI: 10.1369/jhc.4A6592.2005

p38 MAPK via Src, an important upstream signaling factor for actin polymerization, whereas PAR_1 was unable to activate Src, indicating the involvement of a different signal activation cascade in p38 MAPK (Sabri et al. 2003). Additionally, for example, PAR_1 activated p38 MAPK was reported to induce cell proliferation in microglia (Suo et al. 2002) and in smooth muscle cells (Ghosh et al. 2002), showing MAPK activity toward the cell proliferation. These differences in PAR-p38 MAPK signaling events may explain the differences in PAR_4 and PAR_1 induced actin fiber formation. Interestingly, expression level of Hsp27, a factor downstream of p38 MAPK, was suppressed in GYPGQV treated cells, whereas control and SFLLRN treated cells showed similar expression of Hsp27. Thus, our results strongly implied a distinct role for PAR_4 in lung microvascular endothelial cells represented by alveolar capillaries.

Similar forms of PAR_4 induced actin fibers were reported under such stimuli as mechanical stretch (Birukov et al. 2003), ICAM-1 cross-linking (Wang and Doerschuk 2001), and vascular endothelial growth factor treatments (Rousseau et al. 1997), which exhibited actin fibers with thick bundles in endothelial cells. The actin fibers formed by these stimuli were involved in cell barrier, neutrophil adherence, and cell migration, respectively. Concurrently, the cytoskeletal remodeling was revealed to be p38 MAPK-dependent in these experiments, reinforcing a link between PAR_4/p38 MAPK induced actin fibers and the physiological events. These evidences further indicate the importance of PAR_4 activation in endothelial cell functions, although quantitative morphometric analysis of actin remodeling in EC cultures, preferably by image analysis, could lend support to our findings.

The importance of PAR4 in lung endothelial cells could be hypothesized from the fact that PAR_4 expression is up-regulated in response to inflammatory stimuli, TNF-α and IL-1α (Hamilton et al. 2001). These factors are highly expressed and are central mediators in the

pathogenesis during pulmonary fibrosis (Piguet et al. 1993; Raines et al. 1989). Thus, PAR_4 might participate, at least in part, in the induction of pulmonary diseases. In these processes, PAR_4 induced actin fiber may play significant roles in permeability control (Kiemer et al. 2002), neutropil migration (Rousseau et al. 1997), adherence (Wang and Doerschuk 2001), and vascular relaxation (Hamilton et al. 2001).

In conclusion, we have demonstrated the expression of PAR_4 in lung vascular endothelial cells and its functional effect on actin fiber formation. The morphology of PAR_4-induced actin fiber was distinct from that of PAR_1-induced actin fiber. The PAR_4-induced actin fiber formation was highly p38 MAPK-dependent, while the inhibition of p38 MAPK had little effect on PAR_1-induced actin formation. These results indicated that PAR_4 might provide unique capabilities that could not be contributed by PAR_1. Further attempts will be required to elucidate the physiological and pathological role of PAR_4 in the lung vascular endothelial cells.

JHC ex*PRESS*
Online publication date May 30, 2005
This article may be cited as DOI: 10.1369/jhc.4A6592.2005

Acknowledgments

This work was supported by grants from the Ministry of Education, Science, Culture, and Sport of Japan and, in part, by a Maruyama Memorial Research Grant, Nippon Medical School, Tokyo, Japan. We wish to acknowledge Seiko Egawa, Department of Molecular Pathology, Institute of Gerontology, Nippon Medical School, for her assistance with laboratory analyses.

Literature Cited

Asokananthan N, Graham PT, Fink J, Knight DA, Bakker AJ, McWilliam AS, Thompson PJ, Stewart GA (2002) Activation of protease-activated receptor (PAR)-1, PAR-2, and PAR-4 stimulates IL-6, IL-8, and prostaglandin E2 release from human respiratory epithelial cells. J Immunol 168:3577-3585

Bahou WF, Kutok JL, Wong A, Potter CL, Coller BS (1994) Identification of a novel thrombin receptor sequence required for activation-dependent responses. Blood 84:4195-4202

Bayless KJ, Davis GE (2004) Microtubule depolymerization rapidly collapses capillary tube networks in vitro and angiogenic vessels in vivo through the small GTPase Rho. J Biol Chem 279:11686-11695

Birukov KG, Jacobson JR, Flores AA, Ye SQ, Birukova AA, Verin AD, Garcia JG (2003) Magnitude-dependent regulation of pulmonary endothelial cell barrier function by cyclic stretch. Am J Physiol Lung Cell Mol Physiol 285:L785-797

Birukova AA, Birukov KG, Smurova K, Adyshev D, Kaibuchi K, Alieva I, Garcia JG, Verin AD (2004) Novel role of microtubules in thrombin-induced endothelial barrier dysfunction. Faseb J 18:1879-1890

Bretschneider E, Kaufmann R, Braun M, Nowak G, Glusa E, Schror K (2001) Evidence for functionally active protease-activated receptor-4 (PAR-4) in human vascular smooth muscle cells. Br J Pharmacol 132:1441-1446

Carney DH, Mann R, Redin WR, Pernia SD, Berry D, Heggers JP, Hayward PG, Robson MC, Christie J, Annable C, et al. (1992) Enhancement of incisional wound healing and neovascularization in normal rats by thrombin and synthetic thrombin receptor-activating

peptides. J Clin Invest 89:1469-1477

Covic L, Singh C, Smith H, Kuliopulos A (2002) Role of the PAR4 thrombin receptor in stabilizing platelet-platelet aggregates as revealed by a patient with Hermansky-Pudlak syndrome. Thromb Haemost 87:722-727

Faruqi TR, Weiss EJ, Shapiro MJ, Huang W, Coughlin SR (2000) Structure-function analysis of protease-activated receptor 4 tethered ligand peptides. Determinants of specificity and utility in assays of receptor function. J Biol Chem 275:19728-19734

Fujiwara M, Jin E, Ghazizadeh M, Kawanami O (2004) Differential expression of protease-activated receptors 1, 2, and 4 on human endothelial cells from different vascular sites. Pathobiology 71:52-58

Gerszten RE, Chen J, Ishii M, Ishii K, Wang L, Nanevicz T, Turck CW, Vu TK, Coughlin SR (1994) Specificity of the thrombin receptor for agonist peptide is defined by its extracellular surface. Nature 368:648-651

Ghosh SK, Gadiparthi L, Zeng ZZ, Bhanoori M, Tellez C, Bar-Eli M, Rao GN (2002) ATF-1 mediates protease-activated receptor-1 but not receptor tyrosine kinase-induced DNA synthesis in vascular smooth muscle cells. J Biol Chem 277:21325-21331

Hamilton JR, Frauman AG, Cocks TM (2001) Increased expression of protease-activated receptor-2 (PAR2) and PAR4 in human coronary artery by inflammatory stimuli unveils endothelium-dependent relaxations to PAR2 and PAR4 agonists. Circ Res 89:92-98

Henriksen RA, Hanks VK (2002) PAR-4 agonist AYPGKF stimulates thromboxane production by human platelets. Arterioscler Thromb Vasc Biol 22:861-866

Houliston RA, Keogh RJ, Sugden D, Dudhia J, Carter TD, Wheeler-Jones CP (2002) Protease-activated receptors upregulate cyclooxygenase-2 expression in human endothelial

cells. Thromb Haemost 88:321-328

Ishihara H, Connolly AJ, Zeng D, Kahn ML, Zheng YW, Timmons C, Tram T, Coughlin SR (1997) Protease-activated receptor 3 is a second thrombin receptor in humans. Nature 386:502-506

Kahn ML, Hammes SR, Botka C, Coughlin SR (1998a) Gene and locus structure and chromosomal localization of the protease-activated receptor gene family. J Biol Chem 273:23290-23296

Kahn ML, Zheng YW, Huang W, Bigornia V, Zeng D, Moff S, Farese RV, Jr., Tam C, Coughlin SR (1998b) A dual thrombin receptor system for platelet activation. Nature 394:690-694

Kataoka H, Hamilton JR, McKemy DD, Camerer E, Zheng YW, Cheng A, Griffin C, Coughlin SR (2003) Protease-activated receptors 1 and 4 mediate thrombin signaling in endothelial cells. Blood 102:3224-3231

Kawabata A, Kuroda R, Nakaya Y, Kawai K, Nishikawa H, Kawao N (2001) Factor Xa-evoked relaxation in rat aorta: involvement of PAR-2. Biochem Biophys Res Commun 282:432-435

Kiemer AK, Weber NC, Furst R, Bildner N, Kulhanek-Heinze S, Vollmar AM (2002) Inhibition of p38 MAPK activation via induction of MKP-1: atrial natriuretic peptide reduces TNF-alpha-induced actin polymerization and endothelial permeability. Circ Res 90:874-881

Kouklis P, Konstantoulaki M, Vogel S, Broman M, Malik AB (2004) Cdc42 regulates the restoration of endothelial barrier function. Circ Res 94:159-166

Lan RS, Stewart GA, Henry PJ (2000) Modulation of airway smooth muscle tone by protease activated receptor-1,-2,-3 and -4 in trachea isolated from influenza A virus-infected mice. Br J Pharmacol 129:63-70

Langer F, Morys-Wortmann C, Kusters B, Storck J (1999) Endothelial protease-activated

receptor-2 induces tissue factor expression and von Willebrand factor release. Br J Haematol 105:542-550

Marin V, Farnarier C, Gres S, Kaplanski S, Su MS, Dinarello CA, Kaplanski G (2001) The p38 mitogen-activated protein kinase pathway plays a critical role in thrombin-induced endothelial chemokine production and leukocyte recruitment. Blood 98:667-673

Molino M, Barnathan ES, Numerof R, Clark J, Dreyer M, Cumashi A, Hoxie JA, Schechter N, Woolkalis M, Brass LF (1997) Interactions of mast cell tryptase with thrombin receptors and PAR-2. J Biol Chem 272:4043-4049

Nystedt S, Emilsson K, Larsson AK, Strombeck B, Sundelin J (1995) Molecular cloning and functional expression of the gene encoding the human proteinase-activated receptor 2. Eur J Biochem 232:84-89

Nystedt S, Emilsson K, Wahlestedt C, Sundelin J (1994) Molecular cloning of a potential proteinase activated receptor. Proc Natl Acad Sci U S A 91:9208-9212

Piguet PF, Ribaux C, Karpuz V, Grau GE, Kapanci Y (1993) Expression and localization of tumor necrosis factor-alpha and its mRNA in idiopathic pulmonary fibrosis. Am J Pathol 143:651-655

Rahman A, True AL, Anwar KN, Ye RD, Voyno-Yasenetskaya TA, Malik AB (2002) Galpha(q) and Gbetagamma regulate PAR-1 signaling of thrombin-induced NF-kappaB activation and ICAM-1 transcription in endothelial cells. Circ Res 91:398-405

Raines EW, Dower SK, Ross R (1989) Interleukin-1 mitogenic activity for fibroblasts and smooth muscle cells is due to PDGF-AA. Science 243:393-396

Rousseau S, Houle F, Landry J, Huot J (1997) p38 MAP kinase activation by vascular endothelial growth factor mediates actin reorganization and cell migration in human

endothelial cells. Oncogene 15:2169-2177

Sabri A, Guo J, Elouardighi H, Darrow AL, Andrade-Gordon P, Steinberg SF (2003) Mechanisms of protease-activated receptor-4 actions in cardiomyocytes. Role of Src tyrosine kinase. J Biol Chem 278:11714-11720

Shapiro MJ, Weiss EJ, Faruqi TR, Coughlin SR (2000) Protease-activated receptors 1 and 4 are shut off with distinct kinetics after activation by thrombin. J Biol Chem 275:25216-25221

Suo Z, Wu M, Ameenuddin S, Anderson HE, Zoloty JE, Citron BA, Andrade-Gordon P, Festoff BW (2002) Participation of protease-activated receptor-1 in thrombin-induced microglial activation. J Neurochem 80:655-666

Vasanji A, Ghosh PK, Graham LM, Eppell SJ, Fox PL (2004) Polarization of plasma membrane microviscosity during endothelial cell migration. Dev Cell 6:29-41

Vergnolle N, Derian CK, D'Andrea MR, Steinhoff M, Andrade-Gordon P (2002) Characterization of thrombin-induced leukocyte rolling and adherence: a potential proinflammatory role for proteinase-activated receptor-4. J Immunol 169:1467-1473

Vouret-Craviari V, Boquet P, Pouyssegur J, Van Obberghen-Schilling E (1998) Regulation of the actin cytoskeleton by thrombin in human endothelial cells: role of Rho proteins in endothelial barrier function. Mol Biol Cell 9:2639-2653

Vu TK, Hung DT, Wheaton VI, Coughlin SR (1991) Molecular cloning of a functional thrombin receptor reveals a novel proteolytic mechanism of receptor activation. Cell 64:1057-1068

Wang Q, Doerschuk CM (2001) The p38 mitogen-activated protein kinase mediates cytoskeletal remodeling in pulmonary microvascular endothelial cells upon intracellular adhesion molecule-1 ligation. J Immunol 166:6877-6884

Xu WF, Andersen H, Whitmore TE, Presnell SR, Yee DP, Ching A, Gilbert T, Davie EW, Foster

JHC ex*PRESS*
Online publication date May 30, 2005
This article may be cited as DOI: 10.1369/jhc.4A6592.2005

DC (1998) Cloning and characterization of human protease-activated receptor 4. Proc Natl

Acad Sci U S A 95:6642-6646

JHC ex*PRESS*
Online publication date May 30, 2005
This article may be cited as DOI: 10.1369/jhc.4A6592.2005

Figure Captions

Figure 1 PAR_4 expression in human lung endothelial cells. Polyclonal anti- PAR_4 antibody was utilized for immunohistochemical staining. (A) Microvessels in the alveolar walls (arrows) show strong PAR_4 staining. (B) A large vessel in the lung shows weak to moderate PAR_4 staining (arrows). (C) Human lymph node tissue shows no reactivity for PAR_4. Scale bars = 40μm.

Figure 2 PAR_4 expressions in HPAEC and HMVEC-L. (A) RT-PCR analysis was performed for PAR_4 mRNA expression. Representative SYBR Green I gel stainings of PAR_4 and GAPDH in HPAEC (lane 1) and HMVEC-L (lane 2) are shown. GAPDH was used for the normalization and detected at uniform levels. (B) PAR_4 expression was also analyzed by Western blot. Cell lysates containing equal amounts of protein were analyzed and detected as described under "Experimental Procedures." Lane1, HPAEC; Lane 2, HMVEC-L.

Figure 3 Actin fiber formation in HPAEC treated with various concentrations of PAR_4 activating peptide, GYPGQV. HPAEC was exposed to 0, 20, 100, and 500 μM of GYPGQV in EBM (0.25% {w/v} BSA). After 30 min of treatment, cells were fixed with 10% (v/v) neutralized formalin solution, and stained with Alexa 488-phalloidin. Lower panels represent higher magnifications. Scale bars = 40μm.

Figure 4 Actin fiber formation induced by GYPGQV. F-actin was detected by Alexa 488-phalloidin in HPAEC (A) and in HMVEC-L (B). YGPGQV and GYPGQV were exposed to each cell type for 15 min at the concentration of 500 μM. Equal volume of vehicle was used for

control treatments. Lower panels represent higher magnifications. Scale bars = 40μm.

Figure 5 PAR_1 activation by α-thrombin and SFLLRN induces actin fiber formation. HPAEC (A) and HMVEC-L (B) were treated with either 2 U/ml α-thrombin or 100 μM SFLLRN for 15 min. After a wash with HBSS, cells were stained with Alexa 488-phalloidin, and viewed under a confocal laser scanning microscopy. Lower panels represent higher magnifications. Scale bars = 40μm.

Figure 6 Activation of p38 MAPK in HPAEC and HMVEC-L stimulated with PAR activating peptides. (A) HPAEC was either stimulated with dH_2O, GYPGQV, YGPGQV, or SFLLRN for 15 min. After a wash, cells were lysed and the activation of p38 MAPK was assessed by Western blot using specific anti-phospho-p38 MAPK and anti-p38 MAPK antibodies. (B) HMVEC-L lysate was prepared from cells stimulated for 5 min, and both phosphorylated p38 MAPK (pp38 MAPK) and p38 MAPK were similarly detected by Western blot. Lane 1 = Control; lane 2 = GYPGQV; lane 3 = YGPGQV, and lane 4 = SFLLRN.

Figure 7 GYPGQV induced actin fiber formation is inhibited by p38 MAPK inhibitor SB203580. (A) Representative confocal laser microscopic images of F-actin in HPAEC, either treated with (upper panels) or without (lower panels) 2.5 μM SB203580. Cells were first pre-incubated with or without SB203580 for 15 min, and then stimulated by dH_2O, GYPGQV, SFLLRN, or α-thrombin in EBM (0.25% {w/v} BSA) with or without SB203580. After 30 min of treatments, F-actin was stained with Alexa 488-phalloidin. Scale bar = 80μm. (B) Suppressive effect of SB203580 on p38 MAPK activity was determined by Western blot analysis. HPAEC,

Online publication date May 30, 2005
This article may be cited as DOI: 10.1369/jhc.4A6592.2005

pre-treated with either 2.5 μM SB203580 or vehicle for 15 min, were further stimulated with GYPGQV or SFLLRN in EBM (0.25% {w/v} BSA) with or without SB203580 for 30 min. After few washes, HPAEC lysates were separated by SDS-PAGE, and pHsp27 and Hsp27 were detected. CBB represented Coomassie Brilliant Blue R-250 gel staining, indicating equal amount of loaded samples.

JHC ex*PRESS*
Online publication date May 30, 2005
This article may be cited as DOI: 10.1369/jhc.4A6592.2005

Figure 1

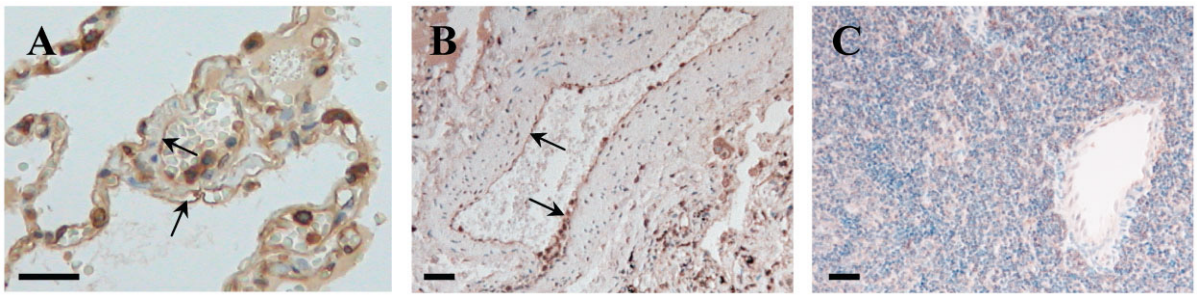

Figure 2

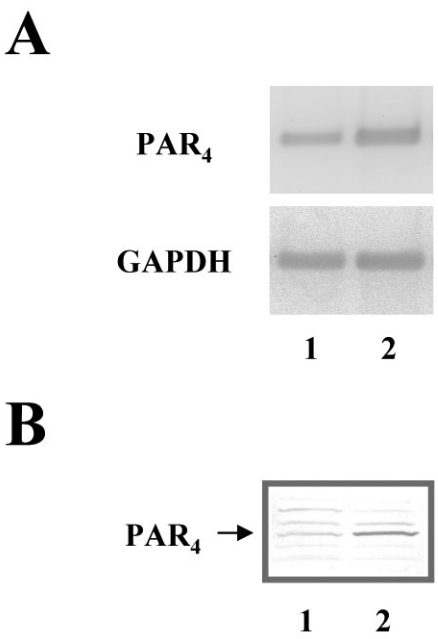

JHC ex*PRESS*
Online publication date May 30, 2005
This article may be cited as DOI: 10.1369/jhc.4A6592.2005

Figure 3

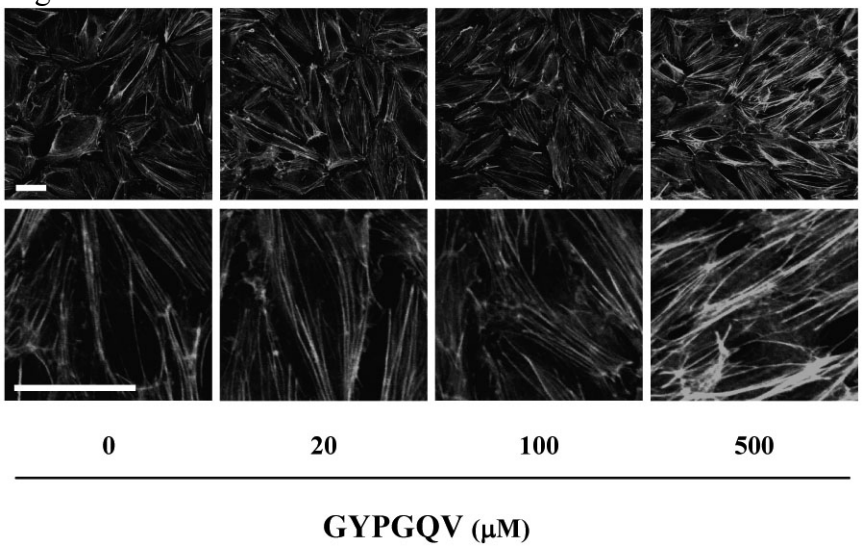

Figure 4

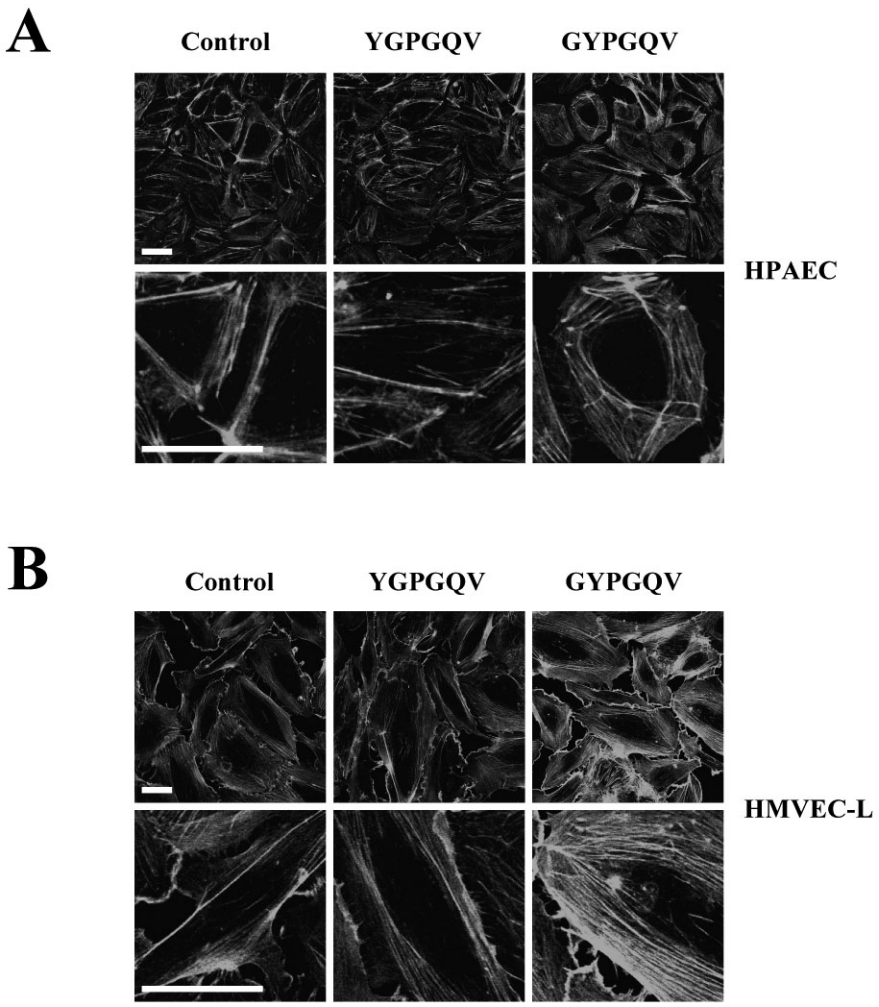

JHC ex*PRESS*
Online publication date May 30, 2005
This article may be cited as DOI: 10.1369/jhc.4A6592.2005

Figure 5

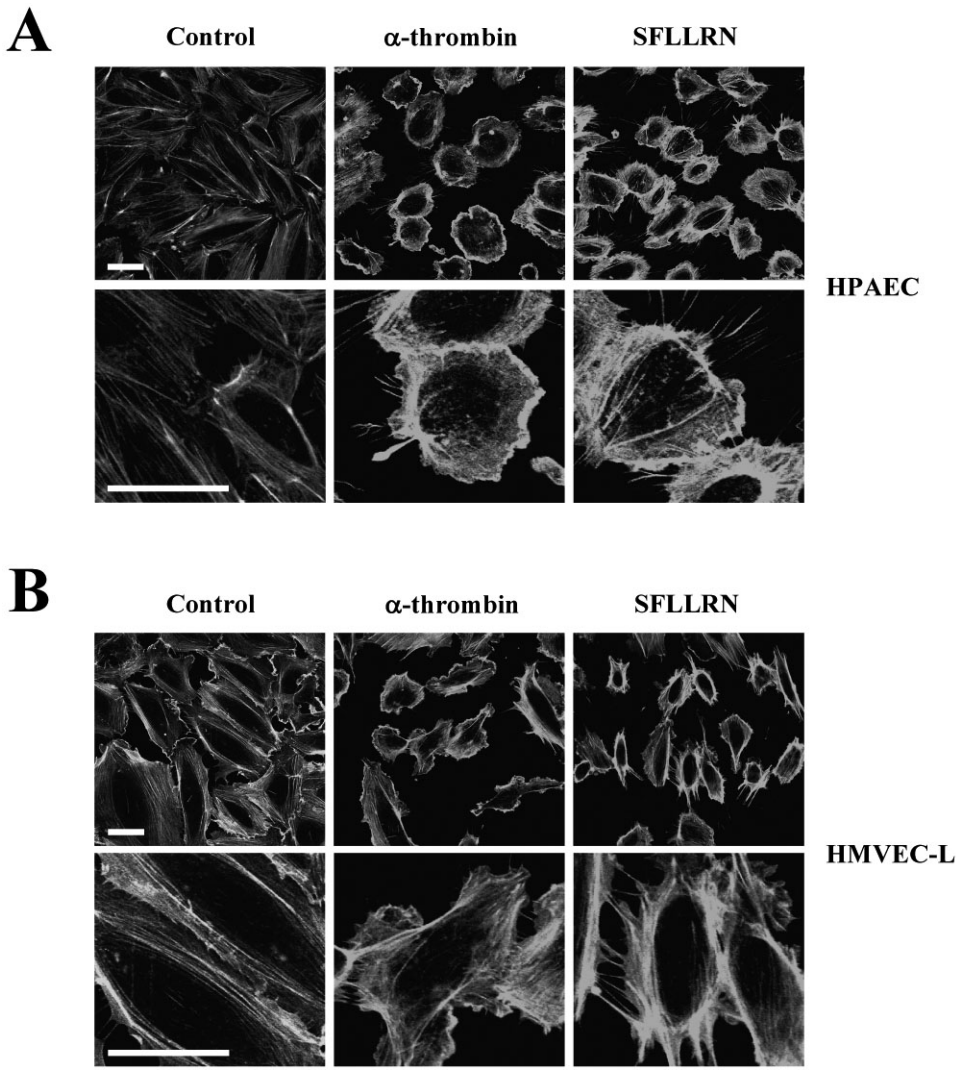

Figure 6

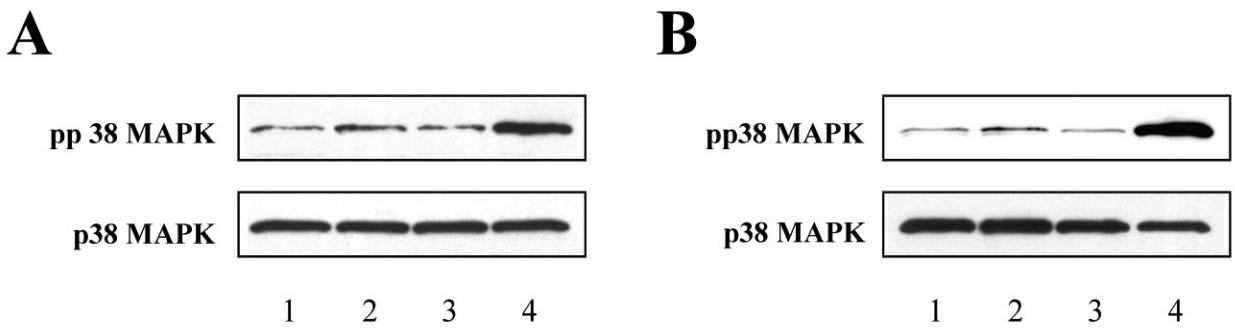

JHC ex*PRESS*
Online publication date May 30, 2005
This article may be cited as DOI: 10.1369/jhc.4A6592.2005

Figure 7